Transport and retention of biogenic selenium nanoparticles in biofilm-coated quartz sand porous media and consequence for elemental mercury immobilization

Wang, Xiaonan; Liu, Bingshen; Pan, Xiangliang; Gadd, Geoffrey Michael

Published in:
Science of the Total Environment

DOI:
10.1016/j.scitotenv.2019.07.309

Publication date:
2019

Transport and retention of biogenic selenium nanoparticles in biofilm-coated quartz sand porous media and consequences for elemental mercury immobilization

Xiaonan Wang [a, b, c, d], Bingshen Liu [b, c], Xiangliang Pan [a, b, *], Geoffrey Michael Gadd [d]

[a] *College of Environment, Zhejiang University of Technology, Hangzhou 310014, China*

[b] *Xinjiang Key Laboratory of Environmental Pollution and Bioremediation, Xinjiang Institute of Ecology and Geography, Chinese Academy of Sciences, Urumqi 830011, China*

[c] *University of Chinese Academy of Sciences, Beijing 100049, China*

[d] *Geomicrobiology Group, School of Life Sciences, University of Dundee, Dundee DD1 5EH, Scotland, UK*

*For correspondence. E-mail panxl@zjut.edu.cn; Tel. +86 571 88320634; Fax +86 571 88320634.

ABSTRACT

Bacterial biofilms are structured cell communities embedded in a matrix of extracellular polymeric substances (EPS) and a ubiquitous growth form of bacteria in the environment. A wide range of interactions between biofilms and nanoparticles have been reported. In the present study, the influence of a mixed bacterial biofilm on retention of biogenic selenium nanoparticles (BioSeNPs) and consequences for immobilization of elemental mercury (Hg^0) in a porous quartz sand system were examined. BioSeNPs were significantly retained in the presence of a biofilm through electrical double layer effects, hydrogen bonding, and hydrophobic, steric and bridging interactions. Moreover, enhanced surface roughness, pore clogging, sieving and entrapment effects mediated by the biofilm also contributed to deposition of BioSeNPs. ~~Whereas~~, thiol groups associated with the biofilm were also involved in ~~is a little helpful for~~ the capture of Hg^0. It is proposed that oxidative complexation between Hg^0 and thiol compounds or S containing organic matter in the biofilm may result in the formation of Hg^{2+}-thiolate complexes and HgS during the binding of Hg^0 with BioSeNPs. The formation of mercury selenide was also involved in Hg^0 immobilization in the porous quartz sand system.

Keywords: Biofilm, Selenium nanoparticles, Hg^0 immobilization, Nanoparticle retention, Thiols, Mercury selenide

Introduction

A bacterial biofilm refers to the multilayer coatings of the cells surrounded by a matrix of extracellular polymeric substances (EPS), such as proteins, extracellular DNA and exopolysaccharide, attached to a living or insert surface (Smirnova et al., 2010). Such biofilms widely occur in natural environments, soil and water-sediment interfaces, and in engineered environments e.g. water treatment systems (Hullebusch et al., 2003). The prevalent formation of a biofilm is highly significant for bacterial growth and survival, and can protect them from harsh environment conditions and antimicrobial agents (Costerton et al., 1995).

Increasing commercial exploitation of nanotechnology, including applications in environmental remediation, has inevitably resulted in the release of nanoparticles (NPs) into the environment which has become an emerging environmental concern. A variety of interactions between NPs and microbial biofilms can occur but efforts to understand them have only just begun. For example, biofilms can influence the formation, adsorption, accumulation, aggregation, biodeterioration and dissolution of NPs. Furthermore, antimicrobial activities of certain NPs have been demonstrated and microbial biofilm communities can be affected (Strathmann et al., 2007; Ikuma et al., 2015). Among the possible interactions, the retention and transport of NPs in the presence of microbial biofilms has received some attention. Transport of polyvinyl alcohol-capped silver nanoparticles (AgNPs) in biofilm-coated porous media was

inhibited because of aggregation, while the retention of poly(vinylpyrrolidone)-stabilized AgNPs in biofilm-coated sand grains was decreased (Choi et al., 2010; Mitzel and Tufenkji, 2014). Tripathi et al. (2011) found that sulfate-functionalized polystyrene latex particles showed increased retention in the presence of a biofilm. The deposition of zero-valent iron NPs, fullerene and ZnO were also all affected strongly by interactions with biofilms in porous media (Tong et al., 2010; Lerner et al., 2012; Jiang et al., 2013). According to previous studies, interactions between NPs and biofilms were closely associated with particle surface chemistry, and the physico-chemical properties of the solution (Shellenberger and Logan, 2002; Leon-Morales et al., 2007). Interactions of NPs with biofilms should therefore be considered as this may not only affect the environmental fate of NPs but also how nanotechnology can be effectively used in environmental applications.

Biogenic selenium nanoparticles (BioSeNPs) have been demonstrated to be effective for elemental mercury (Hg^0) immobilization in groundwater and soil based on the reaction: $Hg^0 + Se^0 \rightarrow HgSe \downarrow$, and the effects of several environmental factors such as dissolved and particulate organic matter, clay minerals and EPS on Hg^0 immobilization efficiency using BioSeNPs have been described in detail (Wang et al., 2018a, b; 2019a ,b). BioSeNPs have been reported to inhibit bacterial growth and the formation of a biofilm because of their

81 antimicrobial properties (Tran et al., 2009; Zonaro et al., 2015). However, the
82 transport and fate of BioSeNPs in the presence of microbial biofilms has not been
83 reported although this is of great interest. If Hg^0 immobilization using BioSeNPs
84 is affected by biofilm interactions such as altered transport of BioSeNPs and Hg
85 binding, this needs to be taken into account in assessing the potential use of NPs
86 for environmental applications. In this study, the effect of a biofilm, comprising
87 a number of bacterial species isolated from natural pond water, on the transport
88 of BioSeNPs was investigated through column transport experiments as well as
89 changes in Hg^0 immobilization efficiency.
90

2. Materials and methods

2.1 Preparation of selenium nanoparticles, groundwater and clean quartz sand

Citrobacter freundii Y9 was used to reduce sodium selenite (1 mM) resulting in the formation of biogenic selenium nanoparticles (BioSeNPs): the BioSeNPs were harvested, purified and freeze-dried according to previous publications (Cui et al., 2016; Wang et al., 2018b). The present study used filtered groundwater taken from Urumqi, Xinjiang, China: details of the filtration method and characterization of the physico-chemical properties of the groundwater are described by Wang et al. (2018b). Quartz sand, purchased from Fuchen Chemical (Tianjin, China), was sieved, washed with concentrated HCl and Milli-Q water, and oven-dried at 550 ^{0}C prior to use in experiments (Wang et al., 2018b).

2.2 Column transport experiments

Transport experiments were carried out using quartz sand porous media in the absence or presence of a bacterial biofilm. To obtain the biofilm coating, quartz sand, sterilized in in a vertical heating pressure stream (LDZX-75KBS, Shanghai, China), was mixed with bacterial suspensions in a flask (at a cell concentration of ~10^{8} cells ml^{-1}) and wet packed into glass cylindrical columns (10 mm inner diameter, 20 cm height) (Long et al., 2009). Bacterial suspensions were obtained by inoculation of pond water, taken near pig farms located in Urumqi, Xinjiang, China, into nutrient broth (Aoboxing Bio-tech Co. Ltd.,

112 Beijing, China). Wet clean quartz sand or quartz sand premixed with bacteria was
113 added to the columns in small increments with 100 μm aperture size nylon mesh
114 placed at the bottom of the columns. During packing, columns were vibrated
115 gently to avoid air entrapment or layering (Tufenkji and Elimelech, 2004). For
116 biofilm-coated quartz sand, nutrient broth was pumped through the columns (1
117 ml min^{-1} flow rate) for 80 h at room temperature, and after the wet packed
118 columns had settled for 5 h, the direction of flow was switched between upflow
119 and downflow every 12 h to make sure that there was a uniform coating of biofilm
120 on the sand (Liu and Li, 2008). For columns packed with clean quartz sand, a
121 similar operation was performed using groundwater instead of nutrient broth.
122
123 After formation of the biofilm, the biofilm-coated quartz sand was subjected
124 to community genomic analysis based on Illumina sequencing (2 × 300 MiSeq
125 platform), the V3–4 region of the bacterial 16S rRNA genes being amplified
126 using 341F-805R primers (Sangon Biotechnology, Shanghai, China). Clean
127 quartz sand and biofilm-coated quartz sand were examined using scanning
128 electron microscopy with energy-dispersive X-ray spectrometry (SEM-EDS)
129 (Zeiss Super 55VP, Oberkochen, Germany). The zeta potential of BioSeNPs,
130 clean quartz sand and quartz sand coated with biofilm in groundwater as a
131 function of pH (3-11) was measured as previously described (Wang et al., 2018b).

After packing, the porosity of the columns was around 0.38. To investigate effects of the biofilm on the transport of BioSeNPs in quartz sand porous media, the columns were first pre-equilibrated with groundwater (100 pore volumes (PVs)), and then equilibrated with sonicated BioSeNPs suspensions (50 mg L^{-1}, 5 PVs) and groundwater (5 PVs). The concentration of BioSeNPs in the influent (C_0) and effluent (C) was determined at regular intervals (0.5 PVs) according to the methods described previously (Wang et al., 2018b). Finally, the clean and biofilm-coated quartz sand were harvested, freeze-dried and examined using SEM-EDS.

2.3 Hg^0 immobilization

The influence of the biofilm in quartz sand porous media on Hg^0 immobilization using BioSeNPs was evaluated in the same columns as used for transport experiments (Fig. S1). After the columns were packed with clean or biofilm-coated quartz sand, they were equilibrated with Hg^0 containing groundwater (10 PVs), and then filled with 2 PVs Hg^0-containing groundwater. The Hg^0 containing groundwater was prepared according to an established protocol (Gai et al., 2016; Wang et al., 2018b). BioSeNPs were added to the columns at a final concentration of 50 mg L^{-1}, and after being kept for one week in a fume hood, the effluent was pumped out and collected at 0.2 PVs intervals for measurement of residual concentrations of Hg^0 and methylmercury (MeHg).

153 Detailed information regarding Hg^0 detection using a mercury analyzer (Lumex
154 RA915+, Saint Petersburg, Russia) has been described previously (Wang et al.,
155 2018b). Hg species in solution were determined using Liquid Chromatography-
156 Hydride Generation Atomic Fluorescence Spectrometry (LC-HGAFS) (Jitian,
157 Beijing, China). After the experiments, the quartz sand with or without attached
158 biofilm was freeze-dried for SEM-EDS and X-ray diffract~~ometer~~ion (XRD) (Bruker
159 D8, Karlsruhe, Germany) analysis. The biofilm-coated quartz sand with addition
160 of BioSeNPs was also characterized using X-ray photoelectron spectroscopy
161 (XPS) (Thermo Fisher Scientific, Waltham, MA, USA) ~~after experiment~~
162 according to ~~the method described in~~ Wang et al. (2017). Another experimental
163 group was carried out without addition of BioSeNPs to the clean quartz sand column: ~~and~~ the
164 quartz sand was subsequently examined using XRD ~~after experiment~~. Two-way ANOVA was
165 used to examine differences in residual Hg^0 content between treatments and depth
166 of column. Differences and correlations were considered statistically significant
167 if $P < 0.05$.
168

3. Results

3.1 BioSeNPs, clean quartz sand, biofilm-coated quartz sand and groundwater

It was demonstrated previously that the BioSeNPs synthesised by *Citrobacter freundii* Y9 through bioreduction of sodium selenite were amorphous selenium nanoparticles which could be applied for effective Hg^0 immobilization (Wang et al., 2017; 2018b). The clean quartz sand particles had smooth clean surfaces (Fig. 1a), while, the surfaces of biofilm-coated quartz sand particles had a coarser appearance since the biofilm was unevenly distributed on the sand particle surfaces (Fig. 1b, c, d).

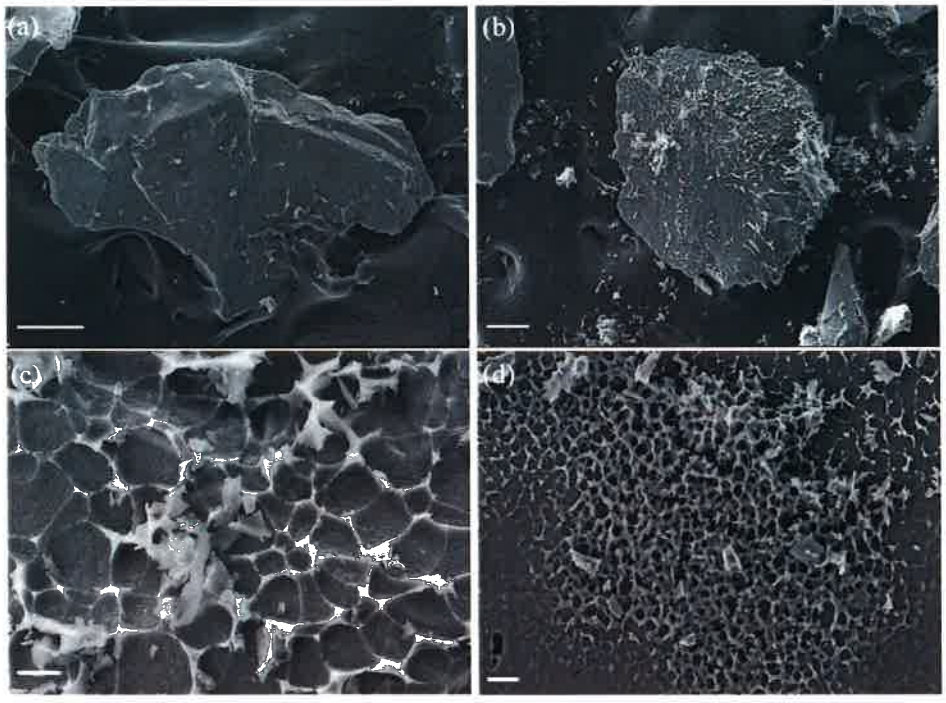

Fig. 1. SEM micrograph of clean quartz sand (a) and biofilm-coated quartz sand (b, c, d). Scale bars: (a, b) 100 μm; (c, d) 10 μm. Typical images are shown from one of several examinations.

In this work, the biofilm was formed by a diversity of bacteria that originated from natural pond water. The taxonomic profile of the biofilm showed that the *Sphingomonas* genus was the most abundant, accounting for 14% of the total (Fig. S2). BioSeNPs, clean quartz sand and biofilm-coated quartz sand all carried a negative charge over the pH range 4-11, and the biofilm coating resulted in the quartz sand becoming less negatively charged. The magnitude of the zeta potential was in the order BioSeNPs < biofilm-coated quartz sand < clean quartz sand (Fig. S3). The physico-chemical properties of the groundwater are listed in Table S1.

3.2 Column transport experiments

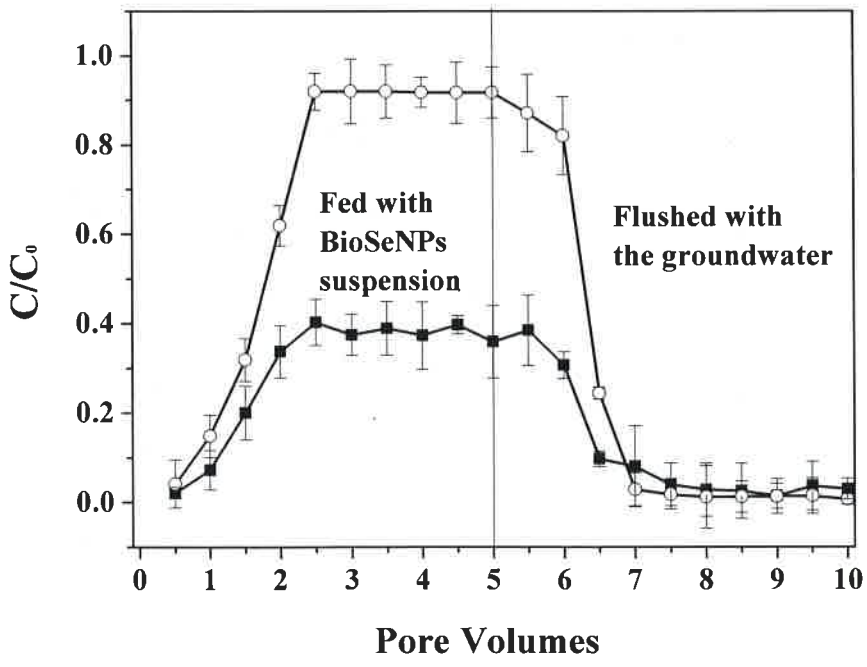

194 Fig. 2. Breakthrough curves of BioSeNPs in clean quartz sand and biofilm-coated
195 quartz sand. Symbols represent: (■) biofilm-coated quartz sand; (○) clean
196 quartz sand. Error bars represent the standard deviation (n=3).

197

198 The breakthrough curves for quartz sand with or without a biofilm coating
199 are shown in Fig. 2. After injection with BioSeNPs suspensions, the value of C/C_0
200 for clean quartz sand increased gradually to ~0.91-0.92 and reached a plateau
201 after equilibration with 2.5 PVs BioSeNPs. However, the biofilm coating lowered
202 the steady-state breakthrough plateau to ~0.37-0.40. The amount of BioSeNPs
203 retained in the columns was calculated through integration of the breakthrough
204 curves. It was found that the retention of BioSeNPs in biofilm-coated quartz sand
205 was ~1.9 times higher than for the clean quartz sand during the period of
206 BioSeNPs injection. When flushed with groundwater, the amount of BioSeNPs
207 leached out of the columns in the absence of a biofilm was ~1.5 times higher than
208 the value recorded in the presence of a biofilm. In other words, BioSeNPs
209 retention in biofilm-coated quartz sand was ~3.0 times higher than that for clean
210 quartz sand. Less BioSeNPs remained on the smooth surfaces of clean quartz sand
211 compared with coarser biofilm-coated sand (Fig. 3).

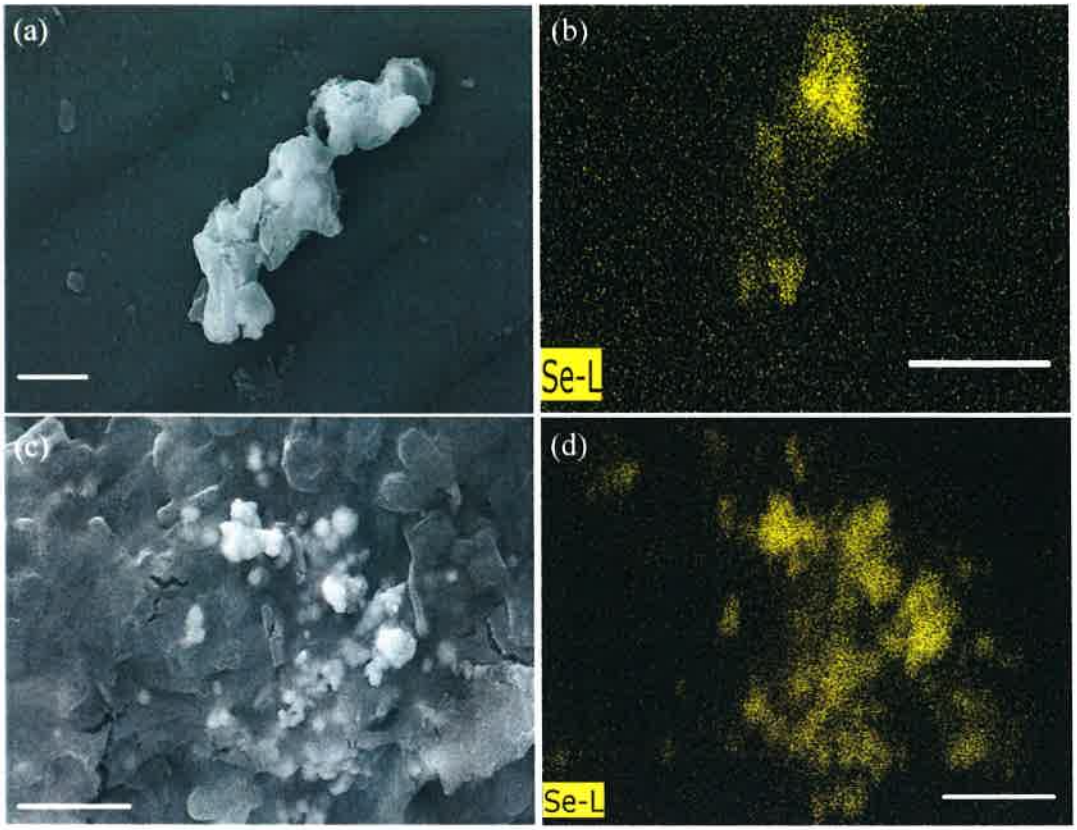

212

213 Fig. 3. SEM micrographs of BioSeNPs retained on clean quartz sand (a) and
214 BioSeNPs remaining on biofilm-coated quartz sand (c). Elemental mapping of Se
215 in clean quartz sand (b) and biofilm-coated quartz sand (d). Scale bars: 2 μm.
216 Typical images are shown from one of several determinations.

217

218 3.3 Hg^0 immobilization

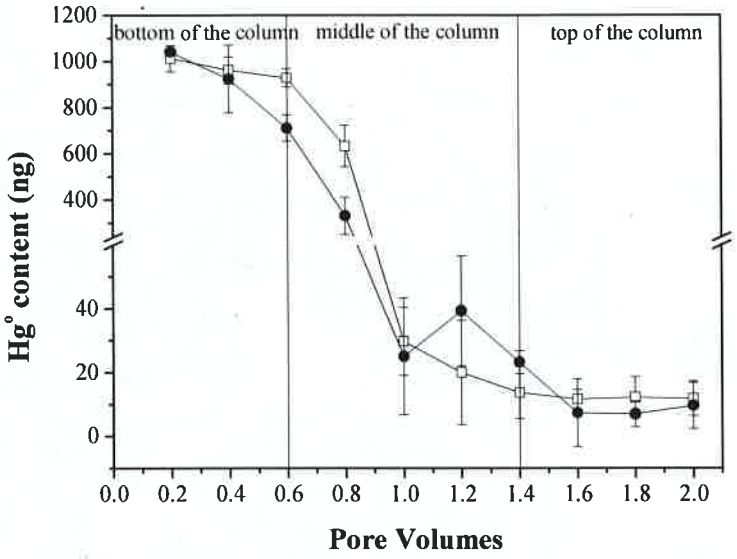

219

220 Fig. 4. Residual mercury content remaining in the quartz sand columns after
221 treatment with BioSeNPs. Samples were taken at 0.2 PVs intervals for
222 measurement. Symbols represent: (□) column packed with clean quartz sand,
223 (●) column filled with biofilm-coated quartz sand. Error bars represent the
224 standard deviation (n=3).

225

226 The residual Hg^0 content remaining in the groundwater after treatment with
227 BioSeNPs in the absence or presence of a biofilm is shown in Fig. 4. ANOVA
228 analysis revealed that the residual Hg^0 content in groundwater was significantly
229 influenced by the biofilm and column depth ($P < 0.05$). At the bottom of the
230 column (0.2-0.6 PVs), the residual Hg^0 content ranged from 710.7 to 1042.5 ng.
231 However, the residual Hg^0 content significantly decreased to 13.7-632.9 ng in the
232 middle of the column (0.8-1.4 PVs). At the top of the column (1.6-2.0 PVs), only

6.9-12.2 ng of Hg^0 remained in the groundwater. It was also found that the amount of residual Hg^0 remaining in the column without biofilm was slightly higher than that for the biofilm-coated column which means the Hg^0 capture efficiency was better in the presence of biofilm than in clean quartz sand at the same depth.

The precipitate formed in the absence or presence of a biofilm was mainly composed of Hg and Se (Fig. S4, 5) and XRD ~~data~~ analysis demonstrated the formation of HgSe and HgS in the presence of a biofilm (Fig. 6a). However, only HgSe was detected in the absence of a biofilm after being treated with BioSeNPs. For the biofilm-coated column without addition of BioSeNPs, a HgS precipitate was also detected (Fig. 6b). Small Hg^0 droplets were observed in the clean quartz sand filled column, but these were not found in the biofilm-coated column. Moreover, S was an obvious element occurring in the precipitate formed in the presence of the biofilm, and the elemental distribution of Hg, Se and S were almost the same. Fig. 7 shows the high-resolution XPS spectrum. The high-resolution spectrum of C 1s exhibits three main peaks, and these binding energy peaks were attributed to C-C, C-O and C=O ~~respectively~~ (Xia et al., 2019). The binding energy peak at 163.8 eV was assigned to RSH groups such as thiols and thiophene and S 2p Peak at 164.9 eV was identified as C-S bonds (Zhang et al., 2013; Wu et al., 2017). The binding energy values for Se^0 at Se 3d5/2 (54.5 eV) and Se 3d3/2 (55.2 eV) were in accordance with ~~those~~ values reported in the literature (Miyake et al., 1984). The mercury peaks at 100.3 and 104.4 eV were attributed to Hg $4f_{7/2}$ and Hg $4f_{5/2}$,

254 which demonstrates that mercury was existed as oxidized mercury species

255 instead of Hg^0 (Li et al., 2018).

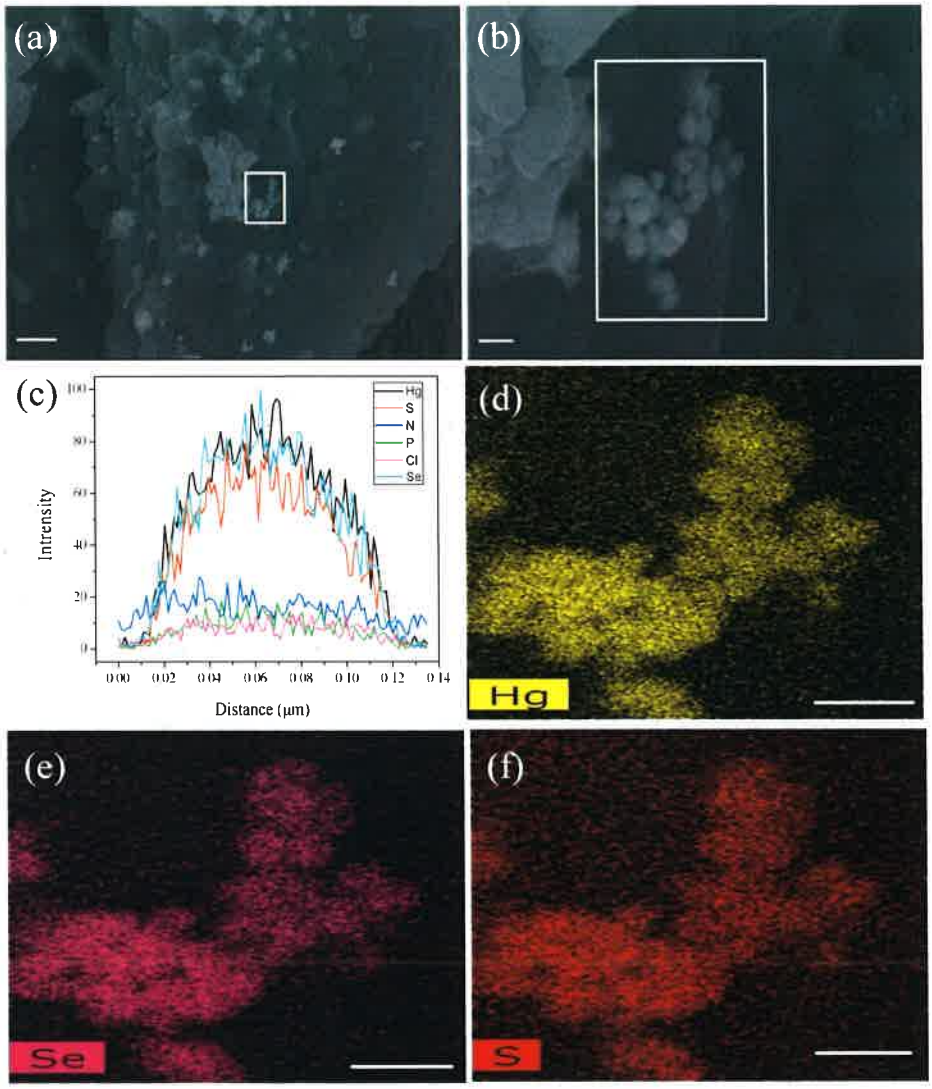

256

257 Fig. 5. Characterization of the precipitate formed in a column filled with biofilm-

258 coated quartz sand after treatment with BioSeNPs. (a, b) SEM micrograph; (c)

259 elemental line scans; elemental mapping scans of (d) Hg, (e) Se and (f) S. Scale

260 bars: (a) 1μm; (b, d, e, f) 200 nm. Typical images are shown from one of several

261 determinations.

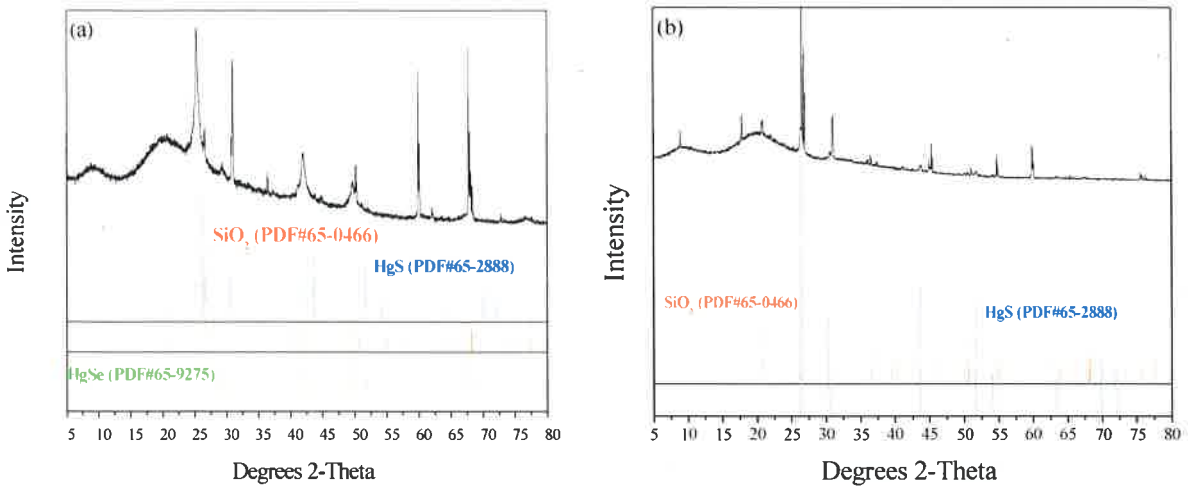

262

263 Fig. 6. XRD pattern of biofilm-coated quartz sand with or without addition of BioSeNPs. Typical patterns are shown.

264

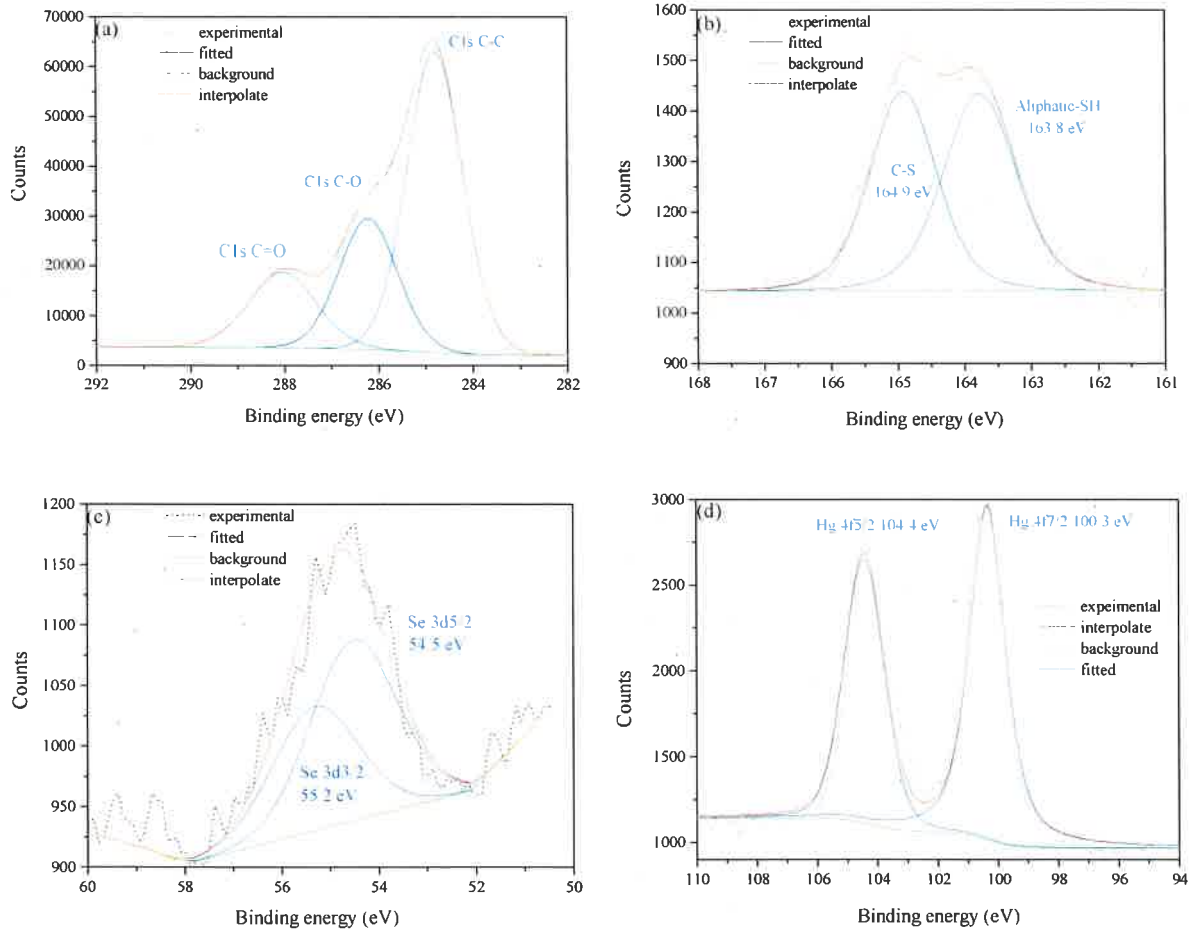

265

266

267 Fig. 7. High resolution XPS spectrum of the biofilm-coated quartz sand in the

268 presence of BioSeNPs and Hg^0. (a) C 1s; (b) S 2p; (c) Se 3d; (d) Hg 4f.

4. Discussion

Single species bacterial biofilms generally do not exist in natural environments. Despite this, much previous work on biofilm effects on transport of NPs in porous media has been carried out with pure culture biofilms comprising one species of bacterium. In this research, the biofilm was multispecies and made up of protecobacteria, bacteroidetes, acidobacteria, actinobacteria, as well as other genera. The retention times for BioSeNPs in the biofilm-coated column was higher than that in the absence of a biofilm, and the presence of the biofilm inhibited the subsequent release of deposited BioSeNPs. This is similar to previous observations where the stability of NPs such as latex particles, CdSe/ZnS quantum dots, fullerene nanoparticles, zero-valent iron nanoparticles and clays was reduced in the presence of a biofilm (Leon-Morales et al., 2007; Tong et al., 2010; Tripathi et al., 2011; Lerner et al., 2012). Electrical double layer effects, hydrogen bonding, and hydrophobic, steric and bridging interactions may all affect the affinity of NPs to a biofilm as well as several other physical and chemical factors (Tong et al., 2010; Lerner et al., 2012).

The porous sand media colonized by the bacterial biofilm possessed a lower negative surface charge compared to control porous media without a biofilm. This is in accordance with a previous report where organic coatings such as a biofilm and ~~the~~ associated EPS decreased the negative surface charge of porous media

290 (Tripathi et al., 2011). It is known that a more negatively charged surface favours
291 the electrical double layer which means that the negatively charged BioSeNPs
292 encounter lower repulsion from the electrical double layer in the biofilm-coated
293 quartz sand. In contrast, decreased retention of poly(vinylpyrrolidone)-stabilized
294 silver NPs in a biofilm-coated sand was found to be a consequence of repulsive
295 electrosteric forces between the biofilm EPS and poly(vinylpyrrolidone) (Mitzel
296 and Tufenkji, 2014).
297
298 Tong et al. (2010) demonstrated that non-DLVO (Derjaguin–Landau–
299 Verwey–Overbeek) forces played a vital role in retention of NPs in the presence
300 of a biofilm. This was associated with ionic strength, and DLVO forces and steric
301 interactions dominating at low and high ionic strengths, respectively (Rijnaarts et
302 al., 1999). A considerable amount of research has reported that steric interactions
303 can play a prominent role in controlling interactions between two polymer
304 covered surfaces (Chen et al., 2008; Pelley et al., 2008). Such steric interactions
305 (polymer-mediated) can be repulsive or attractive (polymer bridging), and these
306 are dependent on the properties of the polymers and the solid surface (Jucker et
307 al., 1998; Kim et al., 2010). Attractive polymer-mediated forces may arise
308 through several mechanisms such as van der Waals interactions, strong ionic or
309 biospecific ligand-receptor bonding and hydrogen bonding (Israelachvili, 2011).
310 In the present study, BioSeNPs were coated with EPS, and the steric interaction

311 could be in the attractive form at certain ionic strengths because of the affinity of
312 biofilm EPS to the polymers on the surface of BioSeNPs (Lerner et al., 2012).
313 Hydrophobic interactions are associated with the attachment of NPs to a
314 biofilm, and this kind of interaction seems to be effective over greater distances
315 (Israelachvili, 2011). It was found that bovine serum albumin-coated glass beads
316 were more likely to retain NPs compared with alginate-coated glass beads, which
317 are less hydrophobic, and the protein/polysaccharide ratio, an indicator of
318 hydrophobicity and hydrophilility, was in accordance with the retention of NPs on
319 the biofilm surface (Xiao and Wiesner, 2013). Hydrogen bonds have also been
320 demonstrated to be an important factor which contributes to retention of NPs. For
321 example, hydrogen bonds mediated the interaction between polysaccharide and
322 TiO_2 and Al_2O_3 particles (Jucker et al., 1997). It was found that *P. aeruginosa*
323 biofilms inhibited the transport of laponite clay particles in a $CaCl_2$ solution,
324 whereas transport was enhanced in a NaCl solution (Leon-Morales et al., 2004,
325 2007). This was because cation bridging between the surface of the biofilm and
326 the NPs could result in more NPs deposition in the presence of Ca^{2+} (Leon-
327 Morales et al., 2007).
328
329 EPS has been reported to account for ~85% of a biofilm mass and this greatly
330 contributes to biofilm formation and development, and also governs attachment
331 of NPs (Smirnova et al., 2010). It is considered that interactions between NPs and

EPS is a critical step for deposition of NPs in biofilm-coated porous media. Tong et al. (2010) showed that biofilm EPS had a great influence on C_{60} deposition using a quartz crystal microbalance technique and dissipation experiments. The components of EPS, such as proteins, would interact with NPs through different attractive interactions (non-DLVO interactions) contributing to retention of NPs (Deguchi et al., 2007). In our previous work, EPS was found to have a great affinity for SeNPs, which would also be helpful for retention of NPs (Wang et al., 2018a).

Surface modification by the biofilm coating has also been associated with enhanced retention of NPs. The "roughness" of quartz sand was increased due to the biofilm coating and a much rougher surface would result in greater retention of NPs (Shellenberger and Logan, 2002; Liu and Li, 2008; Tong et al., 2010). One explanation is that the coating of biofilm supplied more sites of charge heterogeneity leading to increased attachment (Lerner et al., 2012). Furthermore, NPs are likely to be trapped in pores of the biofilm, pore clogging and resultant physical effects significantly contributing to retention of NPs (Ivanov et al., 2004). The formation of biofilm decreased the pore spaces and provided more pore throats and grain-to-grain contact which caused the retention of NPs, and the retention of NPs further decreased the pore space and, as a consequence, more NPs were expected to be deposited (Jiang et al., 2013).

353 It was interesting to find that the presence of a biofilm ~~is a little~~ was helpful for
354 the capture of Hg^0, and elemental mapping of Hg, Se and S showed almost the
355 same distribution in the precipitate. XRD showed Hg^0 was immobilized by
356 the BioSeNPs with formation of HgSe, which has been reported in ~~our~~ previous
357 publications (Wang et al. 2017, 2018a). HgS was produced according to XRD data and the biofilm governed this
358 process. XPS data ~~demonstrated~~ revealed the formation of Hg^{2+}-thiolate complexes, which
359 ~~was~~ were associated with the facilitation of Hg^0 removal ~~caused~~ by the biofilm. In previous
360 ~~publications~~ research, ~~huge~~ attention has been paid to the complexation between DOM and
361 Hg^{2+} since S-containing organic complexes have a strong affinity for Hg^{2+} ~~through~~
362 ~~chelating binding~~ (Wu et al., 2017). Organic matter rather than sulfide is more
363 likely to complex with Hg^{2+} in anoxic environments (Ravichandran, 2004).
364 Moreover, ~~the~~ reactions between Hg^0 and DOM (such as thiol compounds) with
365 the formation of Hg-DOM complexes ~~through oxidative complexation as expressed in~~
366 ~~the following reactions~~ have been reported (Gu et al., 2011):

367 $2R\text{-}SH + Hg^0 \rightarrow R\text{-}SH \cdots Hg^0 \cdots HS\text{-}R$ (physicochemical sorption)

368 $R\text{-}SH \cdots Hg^0 \cdots HS\text{-}R \rightarrow R\text{-}S\text{-}Hg^{2+}\text{-}S\text{-}R + 2H^+ + 2e^-$ (ligand-induced oxidative
369 complexation)

370 $R\text{-}S\text{-}S\text{-}R' + Hg^0 \rightarrow Hg^{2+} + R\text{-}S^- + R'\text{-}S^-$

371 $Hg^{2+} + R\text{-}S^- + R'\text{-}S^- \rightarrow R\text{-}S\text{-}Hg^{2+}\text{-}S\text{-}R'$

Colombo et al., (2013, 2014) found reactivity of thiols towards Hg^0 leading to thiol-mediated microbial oxidation of Hg^0. Zheng et al. (2018) also showed that Hg^0 could be oxidised to Hg^{2+} by natural humic acid or thiol compounds. Hg^{2+} has a high affinity with thiol-containing organic ligands such as glutathione, cysteine and dissolved organic matter, resulting in the formation of Hg^{2+}-thiolate complexes or cell-associated HgS. There are two forms of inorganic Hg in DOM: HgS and $Hg(SR)_2$. Hg^{2+}-thiolate complexes can be converted to HgS through dealkylation reactions (Manceau et al., 2015; Enescu et al., 2016; Thomas et al., 2018; Bourdineaud et al., 2019). This is in accordance with the present work, HgS was formed because of the dealkylation.

It was found that Hg complexed to thiolate could reduce the bioavailabity of Hg to zooplankton and fish (Sjoblom et al., 2000; Richards et al., 2011). The complexation between Hg and DOM and formation of HgS were found to reduce available Hg for methylation, however, low-molecular-weight thiols could mediate methylmercury (MeHg) formation by Hg methylation (Hintelmann et al., 2000; Leclerc et al., 2015; Bouchet et al., 2018). Whereas, MeHg and ethyl mercury (EtHg) were not detected in this work. Accordantly, Hu et al. (2013) also reported oxidization of Hg^0 without methylation.

5. Conclusions

The presence of a biofilm enhanced the retention of BioSeNPs in quartz sand porous media. The attractive interactions between biofilm and BioSeNPs and surface modification such as altered surface texture and roughness, clogging of pores and sieving effects caused by biofilm coating contributed to retention of BioSeNPs. The presence of a biofilm was beneficial to Hg^0 capture due to the formation of Hg^{2+}-thiolate compounds, through ~~oxidative~~ complexation ~~and thiolate ligand~~ and HgS during the immobilization of Hg^0 by BioSeNPs.

Conflict of interest

The authors declare no competing financial interest.

Acknowledgements

This work was supported by the National Natural Science Foundation of China (U1503281 and U1403181) and the National Key Research and Development Program of China (2018YFC1802901 and 2018YFC1802902). G. M. Gadd also gratefully acknowledges an award (NE/M01090/1) under the National Environmental Research Council (UK) Security of Supply of Mineral Resources Grant Program: Tellurium and Selenium Cycling and Supply (TeASe). We also acknowledge financial support from the China Scholarship Council and British

411 Council through the UK-China Joint Research and Innovation Partnership Fund
412 PhD Placement Programme to X. Wang (No. 201703780058).

413

414 **References**

415 Bouchet, S., Goñi-Urriza, M., Monperrus, M., Guyoneaud, R., Fernandez, P.,
416 Heredia, C., Tessier, E., Gassie, C., Point, D., Gue´dron, S., Achá, D.,
417 Amouroux, D., 2018. Linking microbial activities and low-molecular-weight
418 thiols to Hg methylation in biofilms and periphyton from high-altitude
419 tropical lakes in the Bolivian Altiplano. Environ. Sci. Technol., 52, 9758-
420 9767.

421 Bourdineaud, J.P., Gonzalez-Rey, M., Rovezzi, M., Glatzel, P., Nagy, K.L.,
422 Manceau, A., 2019. Divalent mercury in dissolved organic matter is
423 bioavailable to fish and accumulates as dithiolate and tetrathiolate complexes.
424 Environ. Sci. Technol., 53, 4880-4891.

425 Chen, K.L., Elimelech, M., 2008. Interaction of fullerene (C_{60}) nanoparticles with
426 humic acid and alginate-coated silica surfaces: measurements, mechanisms,
427 and environmental implications. Environ. Sci. Technol., 42, 7607-7614.

428 Choi, O., Yu, C.P., Fernández, G.E., Hu, Z., 2010. Interactions of nanosilver with
429 *Escherichia coli* cells in planktonic and biofilm cultures. Water Res., 44,
430 6095-6103.

431 Colombo, M.J., Ha, J., Reinfelder, J.R., Barkay, T., Yee, N., 2013. Anaerobic
432 oxidation of Hg(0) and methylmercury formation by *Desulfovibrio*
433 *desulfuricans* ND132. Geochim. Cosmochim. Acta, 112, 166-177.

434 Colombo, M.J., Ha, J., Reinfelder, J.R., Barkay, T., Yee, N., 2014. Oxidation of
435 Hg(0) to Hg(II) by diverse anaerobic bacteria, Chem. Geol., 363, 334-340.
436 Costerton, J.W., Lewandowski, Z., Caldwell, D.E., Korber, D.R., Lappin-Scott,
437 H.M., 1995. Microbial biofilms. Annu. Rev. Microbiol., 49, 711-745.
438 Cui, Y., Li, L., Zhou, N., Liu, J., Huang, Q., Wang, H., Tian, J., Yu, H., 2016. In
439 vivo synthesis of nano-selenium by *Tetrahymena thermophila* SB210.
440 Enzyme Microb. Technol., 95, 185-191.
441 Deguchi, S., Yamazaki, T., Mukai, S.A., Usami, R., Horikoshi, K., 2007.
442 Stabilization of C_{60} nanoparticles by protein adsorption and its implications
443 for toxicity studies. Chem. Res. Toxicol., 20, 854-858.
444 Enescu, M., Nagy, K.L., Manceau, A., 2016. Nucleation of mercury sulfide by
445 dealkylation. Sci. Rep., 6, 39359.
446 Gai, K., Hoelen, T.P., Hsu-Kim, H., Lowry, G.V., 2016. Mobility of four common
447 mercury species in model and natural unsaturated soils. Environ. Sci.
448 Technol., 50, 3342–3351.
449 Gu, B., Bian, Y., Miller, C.L., Dong, W., Jiang, X., Boyle, L.E.A., 2011. Mercury
450 reduction and complexation by natural organic matter in anoxic
451 environments. Proc. Natl. Acad. Sci. U.S.A., 108, 1479-1483.
452 Hintelmann, H., Keppel-Jones, K., Evans, R.D., 2000. Constants of mercury
453 methylation and demethylation rates in sediments and comparison of tracer
454 and ambient mercury availability. Environ. Toxicol. Chem., 19, 2204-2211.

455 Hu, H., Lin, H., Zheng, W., Tomanicek, S.J., Johs, A., Feng, X., Elias, D.A., Liang,
456 L., Gu, B., 2013. Oxidation and methylation of dissolved elemental mercury
457 by anaerobic bacteria. Nat. Geosci., 6, 751.
458 Ikuma, K., Decho, A.W., Lau, B.L., 2015. When nanoparticles meet biofilms—
459 interactions guiding the environmental fate and accumulation of
460 nanoparticles. Front. Microbiol., 6, 591.
461 Israelachvili, J.N, 2011. Intermolecular and Surface Forces, third ed. Academic
462 Press, Oxford.
463 Ivanov, V., Tay, J.H., Tay, S.L., Jiang, H.L., 2004. Removal of micro-particles by
464 microbial granules used for aerobic wastewater treatment. Water Sci.
465 Technol., 50, 147-154.
466 Jiang, X., Wang, X., Tong, M., Kim, H., 2013. Initial transport and retention
467 behaviors of ZnO nanoparticles in quartz sand porous media coated with
468 *Escherichia coli* biofilm. Environ. Pollut., 174, 38-49.
469 Jucker, B.A., Harms, H., Hug, S.J., Zehnder, A.J.B., 1997. Adsorption of bacterial
470 surface polysaccharides on mineral oxides is mediated by hydrogen bonds.
471 Colloids Surf B Biointerfaces, 9, 331-343.
472 Jucker, B.A., Zehnder, A.J., Harms, H., 1998. Quantification of polymer
473 interactions in bacterial adhesion. Environ. Sci. Technol., 32, 2909-2915.
474 Kim, H.N., Walker, S.L., Bradford, S.A., 2010. Macromolecule mediated
475 transport and retention of *Escherichia coli* O157: H7 in saturated porous
476 media. Water Res., 44, 1082-1093.

Leclerc, M., Planas, D., Amyot, M., 2015. Relationship between extracellular low-molecular-weight thiols and mercury species in natural lake periphytic biofilms. Environ. Sci. Technol., 49, 7709-7716.

Leon-Morales, C.F., Leis, A.P., Strathmann, M., Flemming, H.C., 2004. Interactions between laponite and microbial biofilms in porous media: implications for colloid transport and biofilm stability. Water Res., 38, 3614-3626.

Leon-Morales, C.F., Strathmann, M., Flemming, H.C., 2007. Influence of biofilms on the movement of colloids in porous media. Implications for colloid facilitated transport in subsurface environments. Water Res., 41, 2059–2068.

Lerner, R.N., Lu, Q., Zeng, H., Liu, Y., 2012. The effects of biofilm on the transport of stabilized zerovalent iron nanoparticles in saturated porous media. Water Res., 46, 975–985.

Li, J., Liu, Y., Ai, Y., Alsaedi, A., Hayat, T., Wang, X., 2018. Combined experimental and theoretical investigation on selective removal of mercury ions by metal organic frameworks modified with thiol groups. Chem. Eng. J., 354, 790-801.

Liu, Y., Li, J., 2008. Role of *Pseudomonas aeruginosa* biofilm in the initial adhesion, growth and detachment of *Escherichia coli* in porous media. Environ. Sci. Technol., 42, 443-449.

Long, G., Zhu, P., Shen, Y., Tong, M., 2009. Influence of extracellular polymeric

499 substances (EPS) on deposition kinetics of bacteria. Environ. Sci. Technol.,
500 43, 2308-2314.
501 Manceau, A., Lemouchi, C., Enescu, M., Gaillot, A.C., Lanson, M., Magnin, V.,
502 Glatzel, P., Poulin, B.A., Ryan, J.N., Aiken, G.R., Gautier-Luneau, I., Nagy,
503 K.L., 2015. Formation of mercury sulfide from Hg (II)–thiolate complexes
504 in natural organic matter. Environ. Sci. Technol., 49, 9787-9796.
505 Mitzel, M.R., Tufenkji, N., 2014. Transport of industrial PVP-stabilized silver
506 nanoparticles in saturated quartz sand coated with *Pseudomonas aeruginosa*
507 PAO1 biofilm of variable age. Environ. Sci. Technol., 48, 2715-2723.
508 Miyake, I., Tanpo, T., Tatsuyama, C., 1984. XPS study on the oxidation of InSe.
509 Jpn. J. Appl. Phys., 23, 172.
510 Pelley, A.J., Tufenkji, N., 2008. Effect of particle size and natural organic matter
511 on the migration of nano-and microscale latex particles in saturated porous
512 media. J. Colloid Interface Sci., 321, 74-83.
513 Ravichandran, M., 2004. Interactions between mercury and dissolved organic
514 matter—a review. Chemosphere, 55, 319-331.
515 Richards, J.G., Curtis, P.J., Burnison, B.K., Playle, R.C., 2011. Effects of natural
516 organic matter source on reducing metal toxicity to rainbow trout
517 (*Oncorhynchus mykiss)* and on metal binding to their gills. Environ. Toxicol.
518 Chem., 20, 1159-1166.
519 Rijnaarts, H.H., Norde, W., Lyklema, J., Zehnder, A.J., 1999. DLVO and steric
520 contributions to bacterial deposition in media of different ionic strengths.

521 Colloids Surf B Biointerfaces, 14, 179-195.
522 Shellenberger, K., Logan, B.E., 2002. Effect of molecular scale roughness of
523 glass beads on colloidal and bacterial deposition. Environ. Sci. Technol., 36,
524 184-189.
525 Sjoblom, A., Meili, M., Sundbom, M., 2000. The influence of humic substances
526 on the speciation and bioavailability of dissolved mercury and
527 methylmercury, measured as uptake by *Chaoborus larvae* and loss by
528 volatilization. Sci. Total Environ., 261, 115-124.
529 Smirnova, T.A., Didenko, L.V., Azizbekyan, R.R., Romanova, Y.M., 2010.
530 Structural and functional characteristics of bacterial biofilms. Microbiology,
531 79, 413-423.
532 Strathmann, M., Leon-Morales, C.F., Flemming, H.C., 2007. Influence of
533 biofilms on colloid mobility in the subsurface, in: Frimmel, F.H., Von Der
534 Kammer, F., Flemming, H.C. (eds.), Colloidal transport in porous media.
535 Springer, Berlin, pp. 143-173.
536 Thomas, S.A., Rodby, K.E., Roth, E.W., Wu, J., Gaillard, J.F., 2018.
537 Spectroscopic and microscopic evidence of biomediated HgS species
538 formation from Hg (II)–cysteine complexes: implications for Hg (II)
539 bioavailability. Environ. Sci. Technol., 52, 10030-10039.
540 Tong, M., Ding, J., Shen, Y., Zhu, P., 2010. Influence of biofilm on the transport
541 of fullerene (C60) nanoparticles in porous media. Water Res., 44,
542 1094−1103.

543 Tran, P.L., Hammond, A.A., Mosley, T., Cortez, J., Gray, T., Colmer-Hamood,
544 J.A., Shashtri, M., Spallholz, J.E., Hamood, A.N., Reid, T.W., 2009.
545 Organoselenium coating on cellulose inhibits the formation of biofilms by
546 *Pseudomonas aeruginosa* and *Staphylococcus aureus*. Appl. Environ.
547 Microbiol., 75, 3586-3592.
548 Tripathi, S., Champagne, D., Tufenkji, N., 2011. Transport behavior of selected
549 nanoparticles with different surface coatings in granular porous media
550 coated with *Pseudomonas aeruginosa* biofilm. Environ. Sci. Technol., 46,
551 6942−6949.
552 Tufenkji, N., Elimelech, M., 2004. Deviation from classical colloid filtration
553 theory in the presence of repulsive DLVO interactions. Langmuir, 20,
554 10818-10828.
555 van Hullebusch, E.D., Zandvoort, M.H., Lens, P.N., 2003. Metal immobilisation
556 by biofilms: mechanisms and analytical tools. Rev. Environ. Sci. Biotechnol.,
557 2, 9-33.
558 Wang, X., Pan, X., Gadd, G.M., 2019a. Soil dissolved organic matter affects
559 mercury immobilization by biogenic selenium nanoparticles. Sci. Total
560 Environ., 658, 8-15.
561 Wang, X., Song, W., Qian, H., Zhang, D., Pan, X., Gadd, G.M., 2018a.
562 Stabilizing interaction of exopolymers with nano-Se and impact on mercury
563 immobilization in soil and groundwater. Environ. Sci. Nano, 5, 456-466.

564 Wang, X., Wang, S., Pan, X., Gadd, G.M., 2019b. Heteroaggregation of soil
565 particulate organic matter and biogenic selenium nanoparticles for
566 remediation of elemental mercury contamination. Chemosphere; 221, 486-
567 492.

568 Wang, X., Zhang, D., Pan, X., Lee, D.J., Al-Misned, F.A., Golam Mortuza, M.,
569 Gadd, G.M., 2017. Aerobic and anaerobic biosynthesis of nano-selenium for
570 remediation of mercury contaminated soil. Chemosphere, 170, 266–273.

571 Wang, X., Zhang, D., Qian, H., Liang, Y., Pan, X., Gadd, G.M., 2018b.
572 Interactions between biogenic selenium nanoparticles and goethite colloids
573 and consequence for remediation of elemental mercury contaminated
574 groundwater. Sci. Total Environ., 613, 672-678.

575 Wu, T., Wang, G., Zhang, Y., Kong, M., Zhao, H., 2017. Determination of
576 mercury in aquatic systems by DGT device using thiol-modified carbon
577 nanoparticle suspension as the liquid binding phase. New J. Chem., 41,
578 10305-10311.

579 Xia, S., Huang, Y., Tang, J., Wang, L., 2019. Preparation of various thiol-
580 functionalized carbon-based materials for enhanced removal of mercury
581 from aqueous solution. Environ. Sci. Pollut. Res., 26, 8709-8720.

582 Xiao, Y., Wiesner, M.R., 2013. Transport and retention of selected engineered
583 nanoparticles by porous media in the presence of a biofilm. Environ. Sci.
584 Technol., 47, 2246-2253.

585 Zhang, S., Zhang, Y., Liu, J., Xu, Q., Xiao, H., Wang, X., Xu, H., Zhou, J., 2013.
586 Thiol modified Fe_3O_4@ SiO_2 as a robust, high effective, and recycling
587 magnetic sorbent for mercury removal. Chem. Eng. J., 226, 30-38.
588 Zheng, W., Demers, J.D., Lu, X., Bergquist, B.A., Anbar, A.D., Blum, J.D., Gu,
589 B., 2019. Mercury stable isotope fractionation during abiotic dark oxidation
590 in the presence of thiols and natural organic matter. Environ. Sci. Technol.,
591 53, 1853-1862.
592 Zonaro, E., Lampis, S., Turner, R.J., Qazi, S. J.S., Vallini, G., 2015. Biogenic
593 selenium and tellurium nanoparticles synthesized by environmental
594 microbial isolates efficaciously inhibit bacterial planktonic cultures and
595 biofilms. Front. Microbiol., 6, 584.

Wang et al: "Transport and retention of biogenic selenium nanoparticles in biofilm-coated quartz sand porous media and consequences for elemental mercury immobilization"

Thank you for the reviewers' comments on our manuscript: they are of great help for revising and improving our paper. We have studied the comments carefully and have made the relevant corrections. All revisions are marked in red in the revised manuscript. Detailed responses to the reviewers' comments are as follows (the replies are highlighted in blue):

Reviewer #1:

The influence of a mixed bacterial biofilm on retention of BioSeNPs was investigated in this paper. Meanwhile, the effect of it was found that the biogenic selenium nanoparticles in biofilm-coated quartz sand porous media could immobilize the elemental mercury from water. Furthermore, thiol groups could enhance the mercury immobilization. However, it is well known that mercury could react with Se or thiol. So, what are the new phenomenon, mechanism or technology in this paper?

Response: It is known that mercury could react with Se or thiol, however, the influence of a mixed bacterial biofilm on retention of biogenic selenium nanoparticles (BioSeNPs) and consequences for immobilization of elemental mercury (Hg^0) in a porous quartz sand system has not been reported. In the present study, the transport of

BioSeNPs was inhibited by biofilm, but the oxidative complexation between Hg^0 and thiol and the formation of HgS is a little helpful for the capture of Hg^0.

1. In Figure 7, through the comparison between the clean quartz sand and biofilm coated quartz sand, the efficiencies of Hg removal is not obvious, and it is said that thiol groups associated with the surface of the biofilm, the author also pointed that oxidation of Hg^0 to Hg^{2+} by thiol compounds, so Se NPs and thiol groups don't have very good performance for the removal of mercury by this biofilm.

Response: BioSeNPs have a very good performance for the immobilization of Hg^0, ~98.8% of the Hg^0 was captured in the top of the column. The Hg^0 immobilization using BioSeNPs in the presence/absence of biofilm in the bottom of the column were both inhibited, only 2.9-31.9% of the Hg^0 were captured since the transport of BioSeNPs was suppressed as shown in breakthrough curves. However, at the bottom of the column, the oxidative complexation between Hg^0 and thiol compounds in biofilm and the formation of HgS is a little helpful for the capture of Hg^0 compared with clean quartz sand filled column.

2. This work should give the XPS spectrum of the BioSeNPs and after adsorption with Hg^0. The S2p XPS is also needed.

Response: We have characterized the BioSeNPs using SEM-EDS, XRD and TEM in our previous, the particles were amorphous elemental selenium nanoparticles. XRD and XPS were used to demonstrate the formation of HgSe after adsorption of BioSeNPs with Hg^0. In this study, we added XPS spectrum (Fig. 7) according to reviewer's opinion. S 2p high resolution XPS spectrum was also supplied to reveal the

occurrence of thiolate compounds. XRD pattern (Fig. 6) was also given to demonstrate the formation of HgSe and HgS.

3. The Hg^0 adsorption isotherm should be given.

Response: The immobilization of Hg^0 using BioSeNPs has been illustrated in our previous work and introduction based on the reaction: $Hg^0 + Se^0 \rightarrow HgSe\downarrow$

The mechanisms about oxidative complexation between Hg^0 and thiol were given as follows:

$2R\text{-}SH + Hg^0 \rightarrow R\text{-}SH\cdots Hg^0\cdots HS\text{-}R$ (physicochemical sorption)

$R\text{-}SH\cdots Hg^0\cdots HS\text{-}R \rightarrow R\text{-}S\text{-}Hg^{2+}\text{-}S\text{-}R + 2H^+ + 2e^-$ (ligand-induced oxidative complexation)

$R\text{-}S\text{-}S\text{-}R' + Hg^0 \rightarrow Hg^{2+} + R\text{-}S^- + R'\text{-}S^-$

$Hg^{2+} + R\text{-}S^- + R'\text{-}S^- \rightarrow R\text{-}S\text{-}Hg^{2+}\text{-}S\text{-}R'$

4. The whole article is not easily understood.

Response: We corrected the whole manuscript carefully to make it easily understood.

Reviewer #2:

The authors report transport and retention of biogenic selenium nanoparticles in biofilm-coated quartz sand porous media and consequence for elemental mercury immobilization. The method is short of novelty. Thus, it is not acceptable.

Response: Although methods used in the present study are usual or regular methods, the effects of biofilm on BioSeNPs and consequences for Hg^0 immobilization have not been reported. Biofilm is widely spread in the environment, it necessary to evaluate the effects of biofilm which is helpful to well understand the applications of

BioSeNPs for Hg^0 immobilization. It was found that the transport of BioSeNPs was inhibited, but the oxidative complexation between Hg^0 and thiol and the formation of HgS is a little helpful for the capture of Hg^0.

Reviewer #3:

Because biofilm is omnipresent in soil and water environments, it is important to evaluate the effects of biofilm in retention of nanoparticles and consequences for heavy metal immobilization.

The paper "Transport and retention of biogenic selenium nanoparticles in biofilm-coated quartz sand porous media and consequences for elemental mercury immobilization" by Wang et al. is an interesting work with some novel findings, which answered the important questions in the field of bioremediation using nanoparticles. In this work, the authors demonstrated that BioSeNPs were significantly retained by biofilm and the underlying mechanisms were proposed from the perspective of their chemical interaction, physical impediment of transport of NPs. The consequences of BioSeNPs by biofilm for their sequestration capacity of elemental mercury was also evaluated. All these findings are helpful for improvement of bioremediation of Hg using Se nanoparticles.

Generally speaking, this paper was very clearly organized and well written. Its publication can attract wide attention from the scientists in bioremediation and other relevant fields.

Some speculative sentences should be removed from the section of conclusions.

Response: Many thanks for your estimation and we have revised conclusions.

Reviewer #4:

The authors have conducted study on "Transport and retention of biogenic selenium nanoparticles in biofilm-coated quartz sand porous media and consequence for elemental mercury immobilization". The article however can be made more scientifically strong by incorporating some additional analytical studies on nanoparticles characterization and impact of retention of selenium nanoparticles and mercury immobilization of biofilm microbial community.

Some of my following comments may help authors to rework on the MS for possible publication on this subject. Hence the paper needs major revision.

Specific comments

1. It is advisable to further investigate nanoparticles using TEM, XRD etc. after microbial synthesis and after they are immobilized on biofilm. SEM can't revealed information nanoparticles.

Response: In our previous papers we have investigated BioSeNPs using TEM and XRD, and the synthesized nanoparticles were demonstrated to be amorphous selenium nanoparticles which have strong affinity to Hg^0. Thus, we did not add results of TEM and XRD in the present study.

After immobilization, we used XRD and XPS to exam the product. It was found HgS was synthesized in the presence of biofilm with/without addition of BioSeNPs according to XRD. XRD results showed HgSe and HgS were formed in the presence of biofilm after addition of BioSeNPs. XPS spectrum demonstrated that Hg-thiolate complex was also occurred in the presence of biofilm after addition of BioSeNPs.

2. Please do further characterization study to verify formation of Hg^{2+}- thiol complex and mercury- selenide complex.

Response: We added XRD (Fig. 6) and XPS (Fig. 7) analysis to verify formation of Hg^{2+}-thiol complex and mercury- selenide complex.

3. It will be highly useful if author will perform some toxicity study of synthesized selenium nanoparticles on different ecotoxicological model organisms as these nanoparticles are proposed to be used in environmental remediation. Therefor interaction of these nanoparticles with aquatic organism will greatly enhance applicability of present study.

Response: Your advice is very useful, although BioSeNPs are considered as unharmful to organisms, it is still necessary to carry out the toxicity study of BioSeNPs on different ecotoxicological model organisms. We will do this work systematically in the next paper.

4. Changes in nanoparticles properties (size, stability etc.) after they come in contact with natural water sample may be also useful aspect of study.

Response: Yes, it is of great help to take the changes of nanoparticles' properties into consideration after they were added into natural water. In our previous work, we have investigated the effects of extracellular polymeric substances, dissolved and particulate organic matter, clay minerals and salinity on the stability of BioSeNPs. We will continue to do this kind of work in future.

In conclusion, we have attended to all referee's comments and amended the manuscript accordingly. We have justified our approach and conclusions in the detailed responses. We hope the manuscript is now acceptable for publication.

Xiaonan Wang

E-mail: wangxiaonan_cas@163.com

Corresponding author: Xiangliang Pan

E-mail address: panxl@zjut.edu.cn